JPRS-UEE-89-003
9 MAY 1989

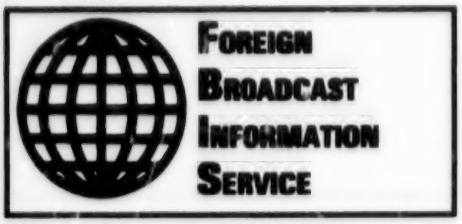

JPRS Report

Science & Technology

USSR: Electronics & Electrical Engineering

Science & Technology
USSR: Electronics and Electrical Engineering

JPRS-UEE-89-003 9 May 1989

CONTENTS

Acoustics, Signal Processing

Method of Calculating Low-Frequency Noise in Measuring Instruments With Correction
[V. N. Malinovskiy, V. P. Fedotov; IZMERITELNAYA TEKHNIKA, No 7, Jul 88] 1
Sound Pressure Transducer With Light-Emitting Diodes
[Ye. S. Avdoshin; IZMERITELNAYA TEKHNIKA, No 7, Jul 88] 1
Geometry of an Interdigital Converter Exciting a Surface Acoustical Wave Waveguide
[O. N. Alifertsev, S. V. Kuzmin, et al.; RADIOTEKHNIKA I ELEKTRONIKA, Vol 33 No 10, Oct 88] 1

Antennas, Propagation

Possibility of Selecting Radio Emission Source by Signal Discrimination on Basis of Wavefront Curvature
[V. V. Nikitchenko, S. N. Gladkikh, et al.; IZVESTIYA VYSSHIKH UCHEBNYKH ZAVEDENIY: RADIOELEKTRONIKA, Vol 31 No 7, Jul 88] 3
Slightly Protruding Weakly Directional Antenna
[V. I. Kornyukhin, S. V. Petrukhin, et al.; IZVESTIYA VYSSHIKH UCHEBNYKH ZAVEDENIY: RADIOELEKTRONIKA, Vol 31 No 7, Jul 88] 3
Shaping Wavefront of Light Pulse and of Control Pulse in Electrooptic Shutters With Large Aperture
[S. L. Afonin, A. A. Golovkov; IZVESTIYA VYSSHIKH UCHEBNYKH ZAVEDENIY: RADIOELEKTRONIKA, Vol 31 No 7, Jul 88] 3
Scattering of Electromagnetic Waves by Metal Cylinder With Annular Magnetic-Dielectric Grating Around It
[V. L. Rudenko; IZVESTIYA VYSSHIKH UCHEBNYKH ZAVEDENIY: RADIOELEKTRONIKA, Vol 31 No 7, Jul 88] 3
RF Loss Analysis of Waveguiding Systems
[I. V. Baryshnikov, V. A. Datskovskiy, et al.; RADIOTEKHNIKA I ELEKTRONIKA Vol 33, No 10, Oct 88] 4
Equivalent Boundary Conditions for a Frequency- Periodic Ribbon Array at the Interface of Two Media
[S. E. Bankov, I. V. Levchenko; RADIOTEKHNIKA I ELEKTRONIKA, Vol 33 No 10, Oct 88] 4
Design of a Cavity Antenna with a Spherical Inner Surface by Means of the Vector Directional Pattern
[Ye. N. Korshunova, A. N. Sivov, et al.; RADIOTEKHNIKA I ELEKTRONIKA, Vol 33 No 10, Oct 88] 4
Equivalent Impedance of Random Irregular Surface in an Inhomogeneous Medium
[N. P Zhuk; RADIOTEKHNIKA I ELEKTRONIKA, Vol 33 No 10, Oct 88] 5

Aerospace, Electronic Systems

Measurement of Stellar Scintillation With Photoelectric Instrument
[A. Ed. Guryanov, Yu. V. Khan; IZVESTIYA AKADEMII NAUK TURKMENSKOY SSR: SERIYA FIZIKO-TEKHNICHESKIKH, KHIMICHESKIKH I GEOLOGICHESKIKH NAUK, No 4, Sep-Oct 88] 6
Characteristics of Radar Measurement of Surface Velocity Distributions
[A. A. Lavrov, B. Ya. Fride; RADIOTEKHNIKA I ELEKTRONIKA, Vol 33 No 10, Oct 88] 6
Properties of One Ranging Algorithm
[I. G. Anikin, N. B. Danilov; RADIOTEKHNIKA I ELEKTRONIKA, Vol 33 No 10, Oct 88] 6

Microwave Theory, Techniques

Method of Complex-Conjugate Matching of Ultrahigh-Frequency Noise Generators
[A. A. Rezchikov, V. G. Kocherga; IZMERITELNAYA TEKHNIKA, No 7, Jul 88] 7
Possibilities of Producing 'Bicomplex' Dielectric Permittivity and Magnetic Permeability Reference Standards for Microwave Measurements
[L. P. Belskaya, O. V. Onishchenko, et al.; IZMERITELNAYA TEKHNIKA, No 7, Jul 88] 7
Gunn Oscillator in Dielectric Mirror Waveguide With Dielectric Disk Cavity
[A. Ya. Kirichenko, V. A. Solodovnik, et al.; IZVESTIYA VYSSHIKH UCHEBNYKH ZAVEDENIY: RADIOELEKTRONIKA, Vol 31 No 7, Jul 88] 7

Coupled Strip Lines and Microstrip Lines With Meandering Gap
[V. M. Lerer, V. D. Ryazanov, et al.; IZVESTIYA VYSSHIKH UCHEBNYKH ZAVEDENIY: RADIOELEKTRONIKA, Vol 31 No 7, Jul 88] 7
Microstrip Phase Shifter on Ferroelectric Film
[S. V. Orlov; IZVESTIYA VYSSHIKH UCHEBNYKH ZAVEDENIY: RADIOELEKTRONIKA, Vol 31 No 7, Jul 88] 8
Application of the Oliner Models to the Case of a Random Microstrip Line Inhomogeneity
[V. M. Alekhin; ELEKTROMEKHANIKA No 8, Aug 88] 8

Communications

Identification of Input Impedances of Wideband Radio Power Channels
[P. L. Asovich, S. A. Zhukov, et al.; IZVESTIYA VYSSHIKH UCHEBNYKH ZAVEDENIY: RADIOELEKTRONIKA, Vol 31 No 7, Jul 88] 9

Components, Hybrids, Manufacturing Technology

Operating Range of Basic Design and Performance Parameters of X-Ray Detectors Made of New Scintillator Materials
[M. Ye. Globus, Ya. A. Valbis; IZMERITELNAYA TEKHNIKA, No 7, Jul 88] 10
Modification of Gummel Method for Solution of Steady-State Problems Pertinent to Modeling of Integrated-Circuit Devices *[A. I. Adamsone, B. S. Polskiy; AVTOMETRIYA, No 3, May-Jun 88]* 10
Calculation of Steady-State Characteristics of Short-Channel MOS-Transistors With Avalanche Multiplication Taken Into Account
[G. V. Gadnyak, S. P. Sinitsa, et al.; AVTOMETRIYA, No 3, May-Jun 88] 10
Modeling Basic Characteristics of VLSI-Devices on MOST-Structures by Static-Charge Method
[V. I. Koldyayev, O. Yu Penzin, et al.; AVTOMETRIYA, No 3, May-Jun 88] 10
Method of Calculating Microwave Parameters of Millimetric-Wave IMPATT-Diodes
[G. Z. Garber; AVTOMETRIYA, No 3, May-Jun 88] 11

Power Engineering

Energy Conservation in Western European Countries
[V. R. Okorokov; PROMYSHLENNAYA ENERGETIKA, No 7, Jul 88] 12
Energy Conservation Activity in Socialist Countries, Part 1
[Yu. A. Tikhomirov, A. M. Mastepanov, et al.; PROMYSHLENNAYA ENERGETIKA, No 7, Jul 88] 12
Comment on Article 'New Electrical Equipment in Standard Modular Cluster Pump Stations for Petroleum Industry' *[V. S. Albokrinov; PROMYSHLENNAYA ENERGETIKA, No 7, Jul 88]* 12

Magnetics

Calculation of Magnetic Systems Fabricated from Materials with Different Magnetic Properties
[V. V. Yakovenko, V. V. Miroshnikov, et al.; ELEKTROMEKHANIKA No 8, Aug 88] 13

Industrial Applications

Gain Calculation for the Optical Unit in the Automatic Control System of the Excavation Unit of Earth-Moving Machinery *[V. A. Lisovin; ELEKTROMEKHANIKA, No 8, Aug 88]* 14
Magnetoelastic Pressure Transducer with Monolithic Sensor and its Mathematical Model
[S. G. Grigoryan; ELEKTROMEKHANIKA, No 8, Aug 88] 14
Calculation of the Acoustic Field from Electrical Discharge in an Underground Cable Line
[A. A. Pirozhnik; ELEKTROMEKHANIKA No 8, Aug 88] 14

Quantum Electronics, Electro-Optics

Error Involved in Determination of Coordinates of Energy Center of Laser Beam During Failure of Matrix-Array Elements in Instrument Transducer
[S. K. Ilin; IZMERITELNAYA TEKHNIKA, No 7, Jul 88] 16
Compensation for Temperature Dependence of Spectral Sensitivity of Photodiode in Pulse-Signal Photometer
[Ye. V. Lesnikov, N. V. Nikitin, et al.; IZMERITELNAYA TEKHNIKA, No 7, Jul 88] 16
Errors of Resonance Ultrasonic Thermometers with Phase Analysis of Echo Signal
[Ya. T. Lutsik, P. G. Stolyarchuk, et al.; IZMERITELNAYA TEKHNIKA, No 7, Jul 88] 16

Study of Optical Fibers With Aid of Thermoplastic Attenuated-Total-Reflectance Elements
[L. N. Kapitanova, V. M. Zolotarev, et al.; OPTIKO-MEKHANICHESKAYA PROMYSHLENNOST, No 6, Jun 88] 88] 16
Effectiveness of Using Circular and Square Fiber Bundles for Visual Search
[Yu. V. Alekseyev, P. A. Mikheyev; OPTIKO-MEKHANICHESKAYA PROMYSHLENNOST, No 6, Jun 88] 17
Determination of Image Converter Characteristics by Methods of Coherent Optics
[V. D. Bakhtin, G. I. Bryukhnevich, et al.; OPTIKO-MEKHANICHESKAYA PROMYSHLENNOST, No 6, Jun 88] 17
X-Ray Image Converter on Microchannel Plates
[A. M. Bonch-Bruyevich, V. N. Ivanov, et al.; OPTIKO-MEKHANICHESKAYA PROMYSHLENNOST, No 6, Jun 88] 17
Holographic Random-Access Memory
[A. P. Grammatin, V. K. Gusev, et al.; OPTIKO-MEKHANICHESKAYA PROMYSHLENNOST, No 6, Jun 88] 17
Instrument for Measuring Losses in Planar Optical Waveguides
[E. A. Arutyunyan, S. Kh. Galoyan, et al.; OPTIKO-MEKHANICHESKAYA PROMYSHLENNOST, No 6, Jun 88] 18
Optical-Grade Polymer Material 'Allur'
[L. B. Vladimirova, I. A. Guseva, et al.; OPTIKO-MEKHANICHESKAYA PROMYSHLENNOST, No 6, Jun 88] 18
Characteristics of InP-MOS Solar Cells at High Density of Solar Radiation Power
[O. Gazakov, A. Kh. Orazberdyyev, et al.; IZVESTIYA AKADEMII NAUK TURKMENSKOY SSR: SERIYA FIZIKO-TEKHNICHESKIKH, KHIMICHESKIKH I GEOLOGICHESKIKH NAUK, No 4, Sep-Oct 88] 18
Thermal Activation Methods of Determining Parameters of Local Levels in Wide-Band Semiconductors
[G. Garyagdyyev; IZVESTIYA AKADEMII NAUK TURKMENSKOY SSR: SERIYA FIZIKO-TEKHNICHESKIKH, KHIMICHESKIKH I GEOLOGICHESKIKH NAUK, No 4, Sep-Oct 88] 19
Design of Electrostatic Deflection Systems Accounting for Deflection Enhancement
[R. A. Lachashvili; RADIOTEKHNIKA I ELEKTRONIKA, Vol 33 No 10, Oct 88] 19
Optical Image Scanning by Acoustic Optic Light Filtering
[V. B. Voloshinov, L. A. Kulakov, et al.; RADIOTEKHNIKA I ELEKTRONIKA, Vol 33 No 10, Oct 88] .. 19

Solid State Circuits

I-E Characteristics and Nonlinear Properties of Indium Phosphide Gunn Diodes in Strong Microwave Fields
[V. I. Borisov, A. L. Galanin, et al.; RADIOTEKHNIKA I ELEKTRONIKA, Vol 33, No 10, Oct 88] 21

UDC 681.335.7.001.24:534.6

Method of Calculating Low-Frequency Noise in Measuring Instruments With Correction

18600009d Moscow IZMERITELNAYA TEKHNIKA in Russian No 7, Jul 88 pp 41-43

[Article by V. N. Malinovskiy and V. P. Fedotov]

[Abstract] An engineering method of calculating the dispersion of low-frequency noise at the output of a measuring instrument with error correction is proposed, this method not being limited to any particular correction algorithm. It is demonstrated on an instrument with a low-pass amplifier or an integrator in the input stage receiving both the signal to be measured and a reference signal through a commutator. Feedback from the instrument output to the commutator through a reference transducer is essential for iterative calculations by a computer on the output side of the instrument and for control of that computer as well as of the instrument and the commutator. Noise originates in the commutator input circuits as well as in the signal source with an internal impedance. Calculations are shown for an instrument with an amplifier or an integrator, an integrator once corrected and one twice corrected with respect to the noise integral being considered. Figures 1; tables 2; references 14: Russian.

UDC 534.2.087.92:681.7.068

Sound Pressure Transducer With Light-Emitting Diodes

18600009g Moscow IZMERITELNAYA TEKHNIKA in Russian No 7, Jul 88 pp 51-52

[Article by Ye. S. Avdoshin]

[Abstract] A sound pressure transducer with light-emitting diodes and fiber optics has been developed and built, its advantages over conventional piezoelectric and electric transducers being its high interference immunity and explosion resistance combined with small size (weight 18 g) and adequate sensitivity. It consists of an LED module (horizontal row of four AI107B light-emitting diodes delivering each 1 mW radiation power at the 850 nm wavelength when conducting a current of 20 mA at a voltage not higher than 2 V) and an optics module (densely packed 16 mm long segments of KVCP-50 quartz fiber, maximum attenuation 3 dB) facing one another under a corrugated acoustic membrane (0.100 mm thick polymer disk 27 mm in diameter). The position of the membrane is adjustable by means of set screws so that an opaque rectangular blind (3.5x9 mm^2) blind made of 0.1 mm thick aluminum foil and glued edgewise to the membrane at the center of the latter can be precisely positioned in the gap of an MBS-9 microscope for position control. The transducer was tested for sensitivity (amplitude)-frequency and other performance characteristics in a Bruehl & Kjoer 4222 anechoic chamber with a 1023 audio-frequency voltage generator and a 2610A amplifier, electric signals energizing a bell and the latter producing pressure on the membrane. The dynamic range of the transducer is 80 dB, with nonlinear distortions not exceeding 2 pct. It was also tested in a VS-68 vibration stand where it withstood sinusoidal vibrations over the 25-80 Hz frequency range with an acceleration of 4g and in a T-1/25 heat chamber where it retained its performance characteristics at temperatures up to 65 deg C. Figures 3; references 5: 4 Russian, 1 Western.

UDC 621.372.826.01

Geometry of an Interdigital Converter Exciting a Surface Acoustical Wave Waveguide

18600101c Moscow RADIOTEKHNIKA I ELEKTRONIKA in Russian Vol 33 No 10, Oct 88 pp 2064-2069

[Article by O. N. Alifertsev, S. V. Kuzmin, and S. A. Fedorov]

[Abstract] This study develops a method of designing a focusing interdigital converter providing maximum gain of the waveguide section by employing an angular spectral analysis to develop the geometry of the interdigital converter in order to achieve effective waveguide excitation. A focusing interdigital converter, which has been demonstrated to be the most effective such device, must create an acoustic field in the cross-sections at the waveguide end that approximates as closely as possible the waveguide modal distribution. The physical problem of optimizing the geometry of a focusing interdigital converter is reduced to determining the converter structure that collects the greatest surface acoustical wave power radiated by the waveguide end. This general problem is divided into two independent stages, the first stage determines the acoustic field radiated by the waveguide at the site of the focusing interdigital converter. The second stage employs the amplitude-phase distribution in the near field of the focusing interdigital converter to determine the converter geometry. The actual process of designing the geometry of a focusing interdigital converter includes selecting the pins to be equiphase surfaces of the waveguide-radiated field and in this case the apodization function must approximate the amplitude distribution as closely as possible. This method is used to calculate the geometry of a focusing interdigital converter for Y-cut lithium niobate for a surface acoustical waveguide with d equals 4λ for distances l equal to 30 and 50 wavelengths. The experimental analysis confirms that the design must include both the pin shapes and the apodization of the pins themselves. Since surface acoustical wave devices are used in a variety of signal processing applications, many different requirements both with respect to the converter aperture and the distance from the converter to the waveguide, the waveguide width, the direction of surface acoustical wave propagation, etc. will be imposed on the focusing interdigital converter. The specifications of the waveguide section that make it possible to select raw

data for designing the waveguide exciter are therefore incorporated to calculate the focusing interdigital converter topology. An analysis of the dependence of the gain on the aperture of the focusing interdigital converter at various lengths suggests that it is possible to achieve a certain prescribed gain at various lengths by appropriate selection of the aperture of the focusing interdigital converter. It is therefore advisable to use the concept of the effective aperture, i.e., the aperture providing the desired gain at a given L. An experimental study was carried out to compare two types of focusing interdigital converters: one developed using a previous topology and one based on the algorithm described in the present study. The analysis revealed the possibility for the practical application of a high-efficiency focusing interdigital converter waveguide exciter with a topology that takes into account the anisotropy of the substrate. The algorithm developed for designing converter topology and the specifications of the waveguide section can be used to excite a wide variety of waveguide designs.

UDC 621.396.677

Possibility of Selecting Radio Emission Source by Signal Discrimination on Basis of Wavefront Curvature

18600010a Kiev IZVESTIYA VYSSHIKH UCHEBNYKH ZAVEDENIY: RADIOELEKTRONIKA in Russian Vol 31 No 7, Jul 88 (manuscript received, after revision, 17 Jun 87) pp 59-62

[Article by V. V. Nikitchenko, S. N. Gladkikh, and P. S. Vikhlyantsev]

[Abstract] Selection of a radio emission source by discrimination between signal and interference on the basis of their wavefront curvatures is analyzed, a linear array of three equidistant identical receiver antennas being the simplest one capable of determining the wavefront curvature. The signal source is assumed to be located on a normal to the receiver line so as to preclude discrimination on the basis of the incidence angle and the receiver array is assumed to be an adaptive one. Its efficiency as discriminator on the basis of wavefront curvature is evaluated analytically in terms of residual interference amplitude and dephasing of the two outer antennas relative to the central one, assuming a receiver array targeted on a source at infinity. Figures 2; references 3: 2 Russian, 1 Western.

UDC 621.396.67

Slightly Protruding Weakly Directional Antenna

18600010b Kiev IZVESTIYA VYSSHIKH UCHEBNYKH ZAVEDENIY: RADIOELEKTRONIKA in Russian Vol 31 No 7, Jul 88 (manuscript received, after revision, 12 May 87) pp 62-63

[Article by V. I. Kornyukhin, S. V. Petrukhin and V. M. Sedov]

[Abstract] The design of an antenna consisting of a strip line, the upper plate a two-dimensionally periodic structure under load and the lower plate a substrate with surface impedance and one-dimensionally periodic surface relief, has been finalized experimentally on the basis of measurements verifying theoretical calculation of the two radiation patterns in the E-plane and in the H-plane respectively. The antenna is well matched to a standard coaxial feeder cable (50 ohms), with a standing-wave ratio of 2.5 over a wide frequency range with a 2.5 ratio of upper cutoff frequency to lower cut-off frequency when its height is equal to one tenth of the nominal wavelength (width-to-height ratio 6.4, length-to-height ration 14). Figures 3; references 3: Russian.

UDC 621.372.55:621.383.6

Shaping Wavefront of Light Pulse and of Control Pulse in Electrooptic Shutters With Large Aperture

18600010c Kiev IZVESTIYA VYSSHIKH UCHEBNYKH ZAVEDENIY: RADIOELEKTRONIKA in Russian Vol 31 No 7, Jul 88 (manuscript received, after revision, 12 Jun 87) pp 62-65

[Article by S. L. Afonin and A. A. Golovkov]

[Abstract] For design and performance analysis of electrooptic shutters with large aperture, theoretical relations are derived for the rise time of a light pulse and the rise time of a controlling voltage pulse in the exit plane of such a shutter. The electrooptica shutter, a cylindrical KDP crystal between the polarizer and the analyzer, carries distributed electrodes in the form of collars around its lateral surface. Calculations are based on both schematic and equivalent-circuit diagrams. Some estimates of subnanosecond rise times are made, considering the difficulty of distortionless generation and transmission of high-voltage pulses with subnanosecond rise time. Figures 2; references 3: Russian.

UDC 621.371.334

Scattering of Electromagnetic Waves by Metal Cylinder With Annular Magnetic-Dielectric Grating Around It

18600010d Kiev IZVESTIYA VYSSHIKH UCHEBNYKH ZAVEDENIY: RADIOELEKTRONIKA in Russian Vol 31 No 7, Jul 88 (manuscript received 28 Apr 87) pp 66-68

[Article by V. L. Rudenko]

[Abstract] Scattering of electromagnetic waves by a metal cylinder with an annular grating of alternately magnetic and dielectric strips wrapped around its lateral surface is considered, specifically diffraction of a plane H-polarized wave. The problem is first solved analytically by superposition of incident an scattered fields in the approximation of the physical theory, assuming that the resultant field at the surface of each strip is the same as at the surface of a metal cylinder with an infinitely long continuous homogeneous layer of a material which has both magnetic permeability and dielectric permittivity wrapped around its lateral surface. The strips are assumed to be lossless, but only in lossy strips with a large pitch-to-wavelength ratio is the interference of natural modes weak so that the analytical solution will be more accurate. The problem is also solved numerically on the basis of partial regions yielding infinite systems of first-order linear algebraic equations readily solvable on a computer by the method of reduction. The results

indicate the possibility of suppressing an image harmonic by designing such a reflector with appropriately matched parameters. Figures 2; references 3: Russian.

UDC 621.372.8.01

RF Loss Analysis of Waveguiding Systems
18600101a Moscow RADIOTEKHNIKA I ELEKTRONIKA in Russian Vol 33 No 10, Oct 88 pp 2029-2034

[Article by I. V. Baryshnikov, V. A. Datskovskiy, and A. V. Upolovnev]

[Abstract] This study employs an electrodynamic analysis to establish the influence of waveguiding structural microroughness on RF loss levels in such systems over a broad range of variation in the microroughness geometry. The RF losses in the waveguiding system are determined by solving the corresponding field problem and satisfying a system of boundary equations. The specific mathematical formulation of the problem made certain implicitly assumptions, including that the field on the microrough surface is independent of the x coordinate, that the bias currents are negligible compared to the conduction currents which is valid in the microwave range and that the eddy currents are induced only in the image plane. The mathematical formulation of the problem makes it impossible to use analytic methods for the solution and hence an approximate analytical method was proposed, involving expansion of the complex contour bounding the calculation region to a canonical contour and introduction of an auxiliary second order boundary condition. Separation of variables is then used to construct a solution of the auxiliary program in the entire "expanded" range. The known field distribution in the conductor can then be used to determine the energy dissipated by the eddy currents in the system and to find the ratio of energies dissipated per unit of length. The entire method was implemented as a Fortran program on a BESM-6 computer. A set of linear algebraic equations with complex variables was solved. The derived functional relations make it possible to analyze the RF losses in the waveguiding systems as a function of the nature of surface roughness and the operating frequency band. The monotonic nature of the curves reflects the frequency dependence of the depth of penetration of the RF field into the metal. At long wavelengths the electromagnetic field penetrates deep into the metal and the microroughness has no substantial influence on RF losses. Accurate to better than 10 percent it is possible to neglect the microroughness when the ratio of the microroughness pitch to the skin-layer depth is less than or equal to 1.25. The plots suggest that the roughness has a more unfavorable influence in metals with a high degree of electrical conductivity. Consistent with the model employed here this phenomenon can be attributed to the insignificant penetration of the RF fields into metals with good conductivity. This in turn produces a greater influence of the microroughness on RF losses in waveguides fabricated from copper.

UDC 621.372.86.01

Equivalent Boundary Conditions for a Frequency-Periodic Ribbon Array at the Interface of Two Media
18600101b Moscow RADIOTEKHNIKA I ELEKTRONIKA in Russian Vol 33, No 10, Oct 88 pp 2045-2050

[Article by S. E. Bankov, I. V. Levchenko]

[Abstract] Generally in analyzing antenna arrays the reflection and transmission coefficients of plane waves striking the array are determined from a solution of the corresponding problem for a Laplace equation. The relation between the electrical and magnetic field components in the various directions from the array is then determined. The present study establishes such a relation, known as the equivalent boundary conditions, for a frequency-periodic ribbon array at the interface of two media by employing the Schwinger transform method to solve integral equations describing the equivalent boundary conditions. In deriving the integral equations the tangential components of the electrical and magnetic fields are written through the electrical and magnetic potentials represented as a Fourier integral. Since the array is infinite, the Fourier transforms of the tangential components are used rather than the components themselves. By employing the boundary conditions for the electrical and magnetic tangential components in the metal and the dielectric a homogeneous set of integral equations for the field components is obtained. Schwinger transforms are used to solve the integral equations. Expressions are then derived for the difference of the tangential magnetic field components in the vicinity of the array. This results in an equivalent boundary condition set for frequency-periodic arrays fabricated from metallic ribbons on the interface of two media. The article concludes with a discussion of the features of electromagnetic phenomena in frequency-periodic ribbon arrays by noting that there are two groups of solutions of Maxwell's equations for such a structure. In the first case the magnetic current in the array slots is equal to zero, and in the second case the electrical current in the array conductors is equal to zero. Changes in the equivalent boundary conditions that occur with different wave types and propagation directions are discussed.

UDC 621.396.67.01

Design of a Cavity Antenna with a Spherical Inner Surface by Means of the Vector Directional Pattern
18600101d Moscow RADIOTEKHNIKA I ELEKTRONIKA in Russian Vol 33 No 10, Oct 88 pp 2070-2075

[Article by Ye. N. Korshunova, A. N. Sivov, and A. D. Shatrov]

[Abstract] The cavity antenna under design is an axiosymmetrical structure formed by a semitransparent spherical surface and an inner impedance body. The

present article presents a method of calculating a resonator where one of the natural resonator modes at a fixed ka has a directional pattern that most closely approximates (in the sense of RMS deviation) a prescribed directional pattern; the cavity Q-factor and the resonant frequency are both given in this case. The calculation result includes the transparency distribution of the spherical surface, the shape of the inner body and the impedance distribution. The analysis is limited to the important practical case of fields with an azimuthal index M equals 1; these include, specifically, unidirectional patterns that do not vanish when θ equals zero. The actual cavity analysis process employs the apparatus developed in a previous study which is based on the natural transparency method for the vector case. It is determined that at sufficiently large ka the transparency of the spherical surface of the cavity may be implemented to be both constant and isotropic. This is supported both by numerical calculations and expressions for the transparency distribution of a sphere. Several different antenna designs with different resonant frequencies, transparency distributions and natural mode directional patterns are analyzed and discussed.

UDC 537.874.2.01

Equivalent Impedance of Random Irregular Surface in an Inhomogeneous Medium

18600101h Moscow RADIOTEKHNIKA I ELEKTRONIKA in Russian
Vol 33, No 10, Oct 88 pp 2194-2197

[Article by N. P. Zhuk]

[Abstract] This study determines the equivalent impedance for a highly conductive, statistically irregular surface of random average shape which is located in a spatially- inhomogeneous medium. The equivalent impedance operator constructed in this case determines the properties of the irregular surface with respect to the mean and fluctuation fields in accordance with nonlocal boundary conditions. The kernel of the equivalent impedance operator includes the correlation function of the irregularities, the irregular surface impedance, the material parameters of the medium and their "tangential" derivatives on the surface as well as the field Green's functions of the regular problem. The analysis indicates that the irregularities on the impedance surface can be taken into account by means of an integrodifferential operator of the impedance surface. The nature of the inhomogeneity was taken into account in "convoluted" form by means of field Green's functions. The equivalent boundary conditions of the impedance type formulated here for the corresponding models of the medium and the surface, which represent particular cases of the model, duplicate existing results.

UDC 520.1.16+525.73

Measurement of Stellar Scintillation With Photoelectric Instrument

18600013a Ashkhabad IZVESTIYA AKADEMII NAUK TURKMENSKOY SSR: SERIYA FIZIKO-TEKHNICHESKIKH, KHIMICHESKIKH I GEOLOGICHESKIKH NAUK in Russian
No 4, Sep-Oct 88 (manuscript received 21 Oct 87) pp 29-34

[Article by A. Ed. Guryanov, Institute of Atmospheric Physics, USSR Academy of Sciences, and Yu. V. Khan, TuSSR Academy of Sciences]

[Abstract] Measurement of stellar scintillation with a photoelectric instrument is considered, specifically measurement of star brightness fluctuations. The instrument designed for this purpose consists of two photomultiplier input channels with a pulse amplifier in each which feeds signals to a ratio-forming circuit, one continuously through a permanent connection and one intermittently through a switch, and a modulus-averaging output channel. In the latter channel a full-wave linear detector on semiconductor diodes is preceded by a wideband filter (lower cutoff frequency 1.4 Hz) and followed by an integrator with a needle indicator. The detector is connected by a switch either only to the ratio-forming circuit when the second photomultiplier channel is also connected to it or only to that second photomultiplier channel when the latter is disconnected from the ratio-forming circuit. The theory of such a measurement and the operation of this instrument match the statistical characteristics of stellar scintillation. The principle of measuring the dispersion of stellar scintillation is demonstrated, with relevant numerical data, on brightness fluctuations of Polaris measured in 1980 from Mt. Dushak-Erekdag. Figures 3; references 3: Russian.

UDC 621.396.969.14

Characteristics of Radar Measurement of Surface Velocity Distributions

18600101e Moscow RADIOTEKHNIKA I ELEKTRONIKA in Russian
Vol 33, No 10, Oct 88 pp 2103-2110

[Article by A. A. Lavrov, B. Ya. Fride]

[Abstract] This study examines the joint temporal and spatial frequency spectrum of a signal received at the aperture of the receive antenna in investigating the characteristics of the radar method for space-time signal processing. This spectral analysis makes it possible to estimate the measurement error in spatial velocity distribution measurements. The accuracy and resolution in radar measurement of the spatial velocity distribution of surface elements are considered. The analysis model is based on a radar set mounted on a support medium traveling rectilinearly at a velocity v and operating in a circular scanning mode. The radar operates in a pulsed mode and the process of image formation in one element at a range of R is analyzed. The pulse repetition frequency provides undistorted transmission of the echo signal spectrum, and the received signal infers its continuous complex envelope. The method of analyzing the radar characteristics is based on an analysis of both the spatial and temporal frequency spectra of the signal at the aperture of the receive antenna. A two-scale model is used to describe the surface and an expression is derived that reflects the spectral density of the spatial and temporal frequencies of the signal reflected from the surface. This expression is represented as a two-dimensional convolution in the frequency domain to assist in both the physical interpretation and for further calculations. Given the radar observation system employed here, the estimate of the spatial velocity distribution of the surface elements is reduced to recovering the function xd(xz) for the derived signal realization of spectrum GP(xz, xt), i.e., it involves the joint estimation of the coordinates of the spectral maximum and the Doppler frequency shift. The velocity measurement accuracy is in fact determined by the spatial frequency measurement accuracy. The expressions suggest that the velocity measurement accuracy depend on the ratio of the angular gradient to the velocity of the radar set. At the same time over a substantial surface area the Doppler frequency shift of the echo signal remains constant and the signal from this region strikes a single Doppler filter. With diminishing velocity of the radar set the measurement accuracy improves, although the range of velocity gradients within which reliable measurement is possible becomes narrower. The analysis suggests that the spatial resolution and velocity measurement accuracy depend on both the radar parameters and the nature of the spatial velocity distribution and may vary significantly over the observation range. The velocity measurement accuracy attained in this case increases with diminishing radar velocity.

UDC 621.396.96.01

Properties of One Ranging Algorithm

18600101i Moscow RADIOTEKHNIKA I ELEKTRONIKA in Russian
Vol 33, No 10, Oct 88 pp 2203-2205

[Article by I. G. Anikin, N. B. Danilov]

[Abstract] The statistical characteristics of ranging to an point source with a known radiation spectrum in a frequency-dependent absorbing medium are calculated by determining the range from the ratio of signal levels measured in two frequency channels. The analysis employs ideal bandpass filters to estimate signal energy within the bandwidth, assumes that the attenuation factor within the band is fixed and that the analysis time satisfies the conditions $\delta fT > 1$. It is determined that if the attenuation level at one frequency is substantially less than that at another frequency the accuracy of the heuristic estimate provided here is approximately two times lower than the accuracy determined by the Cramer-Rao bound.

UDC 621.317.757.089.5.089.6

Method of Complex-Conjugate Matching of Ultrahigh-Frequency Noise Generators
18600009e Moscow IZMERITELNAYA TEKHNIKA in Russian No 7, Jul 88 pp 48-50

[Article by A. A. Rezchikov and V. G. Kocherga]

[Abstract] Complex-conjugate matching of a UHF noise generator to a comparator for calibration against a reference-standard noise generator is considered and adjustment of the matching transformer to minimum power reflection by the tested noise generator is proposed, the tested noise generator reflecting power of the reference generator which has entered the UHF channel of the comparator through a ferrite circulator. The accuracy of such matching is estimated on the basis of relevant scattering matrices. This method is simpler and faster than adjustment of the matching transformer to maximum power transmission through the UHF channel of the comparator, which is especially relevant in the case of low-temperature UHF noise generators. Figures 2; references 3: Russian.

UDC 621.317.411.089.68

Possibilities of Producing 'Bicomplex' Dielectric Permittivity and Magnetic Permeability Reference Standards for Microwave Measurements
18600009f Moscow IZMERITELNAYA TEKHNIKA in Russian No 7, Jul 88 pp 50-51

[Article by L. P. Belskaya, O. V. Onishchenko, and N. L. Yatsynina]

[Abstract] Producing all-Union reference standards of "bicomplex" dielectric permittivity and magnetic permeability covering the 0.2-10 GHz frequency range is discussed from the standpoint of reliable transfer of a unit of each quantity for calibration and inspection. The problem is paucity of available natural or synthetic materials which while having sufficiently stable characteristics at all relevant nominal levels can also be easily shaped, preferably into washers or coaxial cylinders, and properly stored. Few dielectric materials satisfy these requirements and only to a limited extent: quartz and sapphire among the natural ones, polyethylene and corundum ceramic among the synthetic ones. An advantage here is that the real part of their complex permittivity can be theoretically calculated. There are no materials whose magnetic characteristics remain stable in time. These difficulties notwithstanding, "bicomplex" dielectric permittivity and magnetic permeability reference standards have been developed and in 1987 certified for official use. Figures 1; references 5: 4 Russian, 1 Western (in Russian translation).

UDC 621.382.2

Gunn Oscillator in Dielectric Mirror Waveguide With Dielectric Disk Cavity
18600010f Kiev IZVESTIYA VYSSHIKH UCHEBNYKH ZAVEDENIY: RADIOELEKTRONIKA in Russian Vol 31 No 7, Jul 88 (manuscript received, after revision, 27 Jul 87) pp 74-76

[Article by A. Ya. Kirichenko, V. A. Solodovnik and S. N. Kharkovskiy]

[Abstract] The design of an integrated-circuit millimetric-wave Gunn oscillator in a dielectric mirror waveguide with a dielectric disk cavity was checked out experimentally on the basis of measurements at the 8 mm wavelength, with the Gunn diode inside the rectangular waveguide (7.2x10 mm^2 cross-section) made of Teflon-4 on a metal base and with a distributed coupling between this waveguide and a 7.2 mm thick dielectric disk 78 mm in diameter at the location of the diode. The oscillator was tuned electronically and mechanically by moving a metal disk relative to the dielectric one, in the latter case the dependence of the oscillator frequency on the distance between disks having been determined at various levels of the diode supply voltage and at various distances between the waveguide and the parallel to it dielectric disk. Figures 2; references 2: Russian.

UDC 621.372.8.049.75

Coupled Strip Lines and Microstrip Lines With Meandering Gap
18600010g Kiev IZVESTIYA VYSSHIKH UCHEBNYKH ZAVEDENIY: RADIOELEKTRONIKA in Russian Vol 31 No 7, Jul 88 (manuscript received, after revision, 4 Jun 87) pp 79-82

[Article by V. M. Lerer, V. D. F nov and V. A. Sledkov]

[Abstract] Design of coupled strip lines and microstrip lines with a meandering or zigzagging gap between conductors is considered, high directivity being obtained here owing to equalization of even-mode and odd-mode phase velocities. An algorithm of electric and magnetic field calculations in the quasi-static approximation has been programmed in ALGOL-GDR for computer-aided design of such lines on a BESM-6 high-speed machine, both electric and magnetic scalar potentials being given. They are given in the form of series satisfying all boundary conditions at a metal shield (continuity of tangential electric field components E_x,E_z and of normal magnetic field component H_y, symmetry with respect to axis perpendicular to XOZ-plane of geometrical symmetry). The unknown coefficients in these series are determined

from integrodifferential equations for the charge density and the current density respectively, these equations being solved by the Galerkin method. The design of such strip lines and microstrip lines according to this procedure was verified experimentally by measurement of both even-mode and odd-mode retardation coefficients by the resonance method inside a cavity. The lines consisted of two conductors cut from 0.1 mm thick copper foil. The resonance frequency was varied from the lowest f_1 to higher ones f_2 by shortening the cavity, without exceeding the upper limit of the range within which dispersion of the phase velocities remained negligible. While the measured retardation coefficients were only 1.2-3.6 pct smaller than the calculated ones, their ratio differed from the ratio of the calculated ones even less: by 0.94 pct maximum. Figures 3; references 6: 2 Russian, 4 Western.

UDC 621.372.826

Microstrip Phase Shifter on Ferroelectric Film
18600010h Kiev IZVESTIYA VYSSHIKH UCHEBNYKH ZAVEDENIY: RADIOELEKTRONIKA in Russian Vol 31 No 7, Jul 88 (manuscript received, after revision, 3 Jun 87) pp 86-87

[Article by S. V. Orlov]

[Abstract] A microwave phase shifter on a ferroelectric film carried by a dielectric substrate layer carrying a microstrip line on the other surface was designed and built, a higher power rating having been attained by slotting the shielding surface of the microstrip line and a better decoupling of the control circuit from the microwave circuit having been attained by depositing on the ferroelectric film a slotted structure of parallel alternately positive and negative bar electrodes for application of the control voltage. This phase shifter with $(Ba,Sr)TiO_3$ film on a 1 mm thick and 24x30 mm large Policor substrate layer, with four 0.020-0.025 mm wide slots 7 mm apart on the shielding surface, was tested for the frequency characteristics of attenuation and standing-wave ratio without a control voltage and under a control voltage of 200 V, also for the control characteristics at various frequencies within the 3 GHz band at a power level of 10 W continuous without overheating. The estimated power rating of this phase shifter is 50-100 W. The decoupling of its control circuit is at least 30 dB relative to the microwave signal. Figures 2; references 4: Russian.

UDC 621.372.8.049.75

Application of the Oliner Models to the Case of a Random Microstrip Line Inhomogeneity
1860086d Novocherkassk ELEKTROMEKHANIKA in Russian No 8, Aug 88 pp 95-97

[Article by V. M. Alekhin]

[Abstract] Specialists have widely employed the oliner model of a microstrip line to account for inhomogeneities in strip lines due to its simplicity and a level of accuracy of calculation results acceptable for engineering practice. Appropriate test material has not, however, been available for coupled lines containing complex inhomogeneities and this has delayed the broad utilization of the oliner model in computer-aided design of strip devices. This study demonstrates one application of the oliner model to analyzing a single line inhomogeneity. The concept of linear electrical constants is conserved for an inhomogeneous line, although it is more general in nature, making it possible to use telegraph equations in the analysis. Subsequent equations are used to produce a matrix relation between the quantities at the oscillator end of the inhomogeneity and the quantities on its receiving end. The normalized wave impedances at the beginning and end of the inhomogeneity figuring in the matrix expressions are determined within the framework of the oliner model. The formulae suggest that in order to solve the derived integral it is necessary to represent the normalized inhomogeneities width as a function of the x coordinate or to first decompose the inhomogeneity lengthwise into sections and to replace the integral with a corresponding finite sum. More refined calculations account for losses in the conductors of the strip line and the dielectric. This analysis suggests that it is necessary to apply the oliner model to coupled strip lines for computer-aided design of strip devices that takes account of inhomogeneities. A special study will be devoted to this issue.

UDC 621.317.34

Identification of Input Impedances of Wideband Radio Power Channels

18600010e Kiev IZVESTIYA VYSSHIKH UCHEBNYKH ZAVEDENIY: RADIOELEKTRONIKA in Russian Vol 31 No 7, Jul 88 (manuscript received, after revision, 6 Jul 87) pp 71-74

[Article by P. L. Asovich, S. A. Zhukov, V. V. Obrovets and V. V. Polevoy]

[Abstract] Use of a measuring line as an impedance standard for determining the input impedance of metric-wave and decametric-wave radio channels at nominal power levels by comparing the wave impedance of such a load with that of the measuring line is considered, an algorithm of resistance and reactance identification being shown which involves calculation of the voltage across the measuring line at points where it is measured. Identification of the impedance components is treated as a problem of discrepancy minimization, with the mean-square of quasi-Chebyshev difference between calculated and measured complex voltage amplitude as the minimizable functional. The problem is solved by the gradient method of small increments. This identification procedure should be very helpful in the design of wideband radio power channels. Figures 3; references 4: 3 Russian, 1 Western (in Russian translation).

UDC 53.089.5:539.1.(.3:537.531

Operating Range of Basic Design and Performance Parameters of X-Ray Detectors Made of New Scintillator Materials

18600009h Moscow IZMERITELNAYA TEKHNIKA in Russian No 7, Jul 88 pp 54-55

[Article by M. Ye. Globus and Ya. A. Valbis]

[Abstract] Selection of new scintillator materials such as $Y_3Al_3O_{12}$:Ce and $YalO_3$:Ce as gamma-radiation detectors is analyzed from the standpoint of limitations on the basic design and performance parameters, the advantages of these detectors being high time resolution needed for high-speed scanning devices and high chemical stability needed for geological exploration. The basic parameters to be considered are length of the scintillator crystal and range of measurable gamma-radiation energy. The crystal must not be shorter than the energy-dependent mean free path for photons, which is related to the photon absorption coefficient, and its maximum length is limited by reabsorption of its emitted own radiation. The threshold of measurable energy is determined by the detector sensitivity and, inasmuch as detection of higher-energy gamma quanta requires a longer crystal, the maximum measurable energy is limited by the length of the crystal. Calculations for both materials as detectors of gamma quanta within the x-ray range of energy higher than $0.0136Z^2$ keV (Z-effective order number) and much lower than mc^2 equal to 511 keV have been made on the basis of a straight prismatic or cylindrical crystal with a larger than unity length-to-width ratio and correspondingly oriented parallel to the incident gamma flux, all facets assumed to have a mirror polish and the one opposite to the photosensitive one to also have an almost ideally reflective coating. The results are presented in graphical form, as families of crystal length vs minimum measurable energy and crystal length vs maximum measurable energy curves for various values of the absorption coefficient. Figures 2; tables 1; references 7: 4 Russian, 3 Western (1 in Russian translation).

Modification of Gummel Method for Solution of Steady-State Problems Pertinent to Modeling of Integrated-Circuit Devices

18600014a Novosibirsk AVTOMETRIYA in Russian No 3, May-Jun 88 (manuscript received 12 Jun 87) pp 3-7

[Article by A.I. Adamsone and B.S. Polskiy, Riga]

[Abstract] A modification of Gummel's iterative method is proposed for efficient numerical simulation of steady-state relations in integrated-circuit devices, the original method being used for numerical solution of the fundamental system of equations of semiconductor physics but becoming unwieldy and inefficient when applied to a two-dimensional or three-dimensional physical model owing to ill-conditionedness of the continuity equations. Separate solution of each continuity equation in two steps, rough solution in variables n,p by the Buleyev method (N.I. Buleyev, 1970) for initial approximations followed by special linearization, leads to linear systems of difference equations which have symmetric matrices and are solvable by the Meijerink-VanderHorst ICCG method (J.A. Meijerink and H.A. VanderHorst, 1977) rather than to systems of equations with asymmetric matrices obtained by Newton linearization. Fast convergence of this modification is demonstrated on the system of five equations for Jn, Jp, div Jn, div Jp, and potential difference in a transistor structure. Figures 1; tables 4; references 7: 4 Russian, 3 Western.

Calculation of Steady-State Characteristics of Short-Channel MOS-Transistors With Avalanche Multiplication Taken Into Account

18600014b Novosibirsk AVTOMETRIYA in Russian No 3, May-Jun 88 (manuscript received 9 Feb 87) pp 8-13

[Article by G. V. Gadnyak, S. P. Sinitsa and N. L. Shvarts, Novosibirsk]

[Abstract] The current-voltage characteristic of an MOS-transistor, also the potential distribution as well as electron concentration and hole concentration distributions in its structure, were calculated with strong-field effects and avalanche multiplication taken into account. The initial approximation for starting Gummel iterations was selected by assuming an electric field uniform over the distance along which an electron acquires sufficient energy for impact ionization and by assuming a pure drift avalanche current through the substrate. The system of linear equations with a thinned matrix, namely two finite-difference equations of transfer continuity and one quasi-linearized Poisson equation, was solved in the diffusion-drift approximation for a rectangular region with appropriate boundary conditions rather than be the method of incomplete factorization. These are the essential differences between the MOS2 program and the older MOS1 program. Calculations were made on a BESM-6 high-speed computer for a transistor with a 0.002 mm long channel and a substrate having an effective resistance of 9 kohm or 45 kohm, the gate voltage being varied (1-2 V) and the drain voltage being varied (9-10 V) but the voltage across the ohmic contact at the substrate assumed to be zero. The authors thank M.S. Obrekht for assistance in optimization of the MOS2 program and thus shortening the computer time. Figures 7; references 12: 1 Russian, 11 Western.

Modeling Basic Characteristics of VLSI-Devices on MOST-Structures by Static-Charge Method

18600014c Novosibirsk AVTOMETRIYA in Russian No 3, May-Jun 88 (manuscript received 12 Jun 87) pp 16-25

[Article by V.I. Koldyayev, O.Yu. Penzin and O.N. Shakhova, Novosibirsk]

[Abstract] The principle of modeling VLSI-devices in the static-charge approximation is described and the procedure is demonstrated on VLSI-MOST structures. The

modeling process consists of two stages, determination of the two-dimensional distribution of electrostatic potential assuming an equilibrium distribution of static charge followed by determination of key parameters and characteristics on the basis of that distribution. With thermal generation disregarded in the description of both electron and hole concentrations as functions of the electrostatic potential in the state of thermal equilibrium, the two-dimensional Poisson equation is solved for any region of an active and parasitic MOST pair with conditions of symmetry for the electric field intensity at five planes of geometrical symmetry and the Dirichlet boundary conditions at the interface with the common substrate. The algorithms of threshold voltage, reach-through voltage, and reach-through current calculation have been programmed for three extreme cases characterizing two-dimensional approximation: 1) gate width much larger than thickness of space-charge layer, 2) channel length much larger than thickness of space-charge layer, 3) both gate width and channel length much larger than thickness of space-charge layer. Analysis of structures on the basis of computer-aided solution of the Poisson equation for model problems with known analytical solution indicates a high accuracy of the numerical method. Figures 6; references 8: 5 Russian, 3 Western (1 in Russian translation).

Method of Calculating Microwave Parameters of Millimetric-Wave IMPATT-Diodes

18500014d Novosibirsk AVTOMETRIYA in Russian No 3, May-Jun 88 (manuscript received 12 Jun 87) pp 25-28

[Article by G. Z. Garber, Moscow]

[Abstract] A method of calculating the microwave oscillator and amplifier parameters of millimetric-wave IMPATT-diodes by numerical modelling is outlined, such a method being not only less laborious but also more accurate than experimental methods. It is based on a diffusion-drift model which takes thermal inertia of electrons into account and its is an extension of the Scharfetter-Gummel method, with impact ionization coefficients and diffusion coefficients for electrons and holes as well as electron mobility and hole mobility expressed as functions of the electric field intensity. The active region of a diode is described by a system of nine partial differential equations of kinetics in the one-dimensional approximation: one Poisson equation, four equations of electron charge and energy transfer, four equations of hole charge and energy transfer. The initial-value and boundary-value problem for this system of equations is soled by conversion of the equations into their central-difference analogs. Voltage and current as functions of time, together with the area of the p-n junction, yield the microwave parameters of an IMPATT-diode. The computation process continues until it yields a steady-state periodic oscillation mode. Figures 1; references 5: 3 Russian, 2 Western.

UDC 658.26.003(104)

Energy Conservation in Western European Countries

18600008a Moscow PROMYSHLENNAYA ENERGETIKA in Russian No 7, Jul 88 pp 42-43

[Article by V. R. Okorokov, doctor of technical sciences, International Institute of Applied System Analysis (Austria)]

[Abstract] The dynamics of energy conservation in countries of the European Economic Community and other Western European countries over the 1979-86 period have been evaluated in terms of energy efficiency, ratio of energy consumption to energy production, and the relation of both to the dynamics of the gross national product, also in terms of the relation between tons of the petroleum equivalent per million dollars worth of the gross national product and the cost (in dollars) of energy to the consumer per ton of the petroleum equivalent. This evaluation is based on an analysis of three industries: construction materials, steel casting, and aluminum. The goal of energy conservation is defined as strictly optimizing, through regulation and standardization, the design, the production, and the operation of energy-consuming equipment. Figures 2; references 3: Western.

UDC 658.28.003.1(103)

Energy Conservation Activity in Socialist Countries, Part 1

18600008b Moscow PROMYSHLENNAYA ENERGETIKA in Russian No 7, Jul 88 pp 44-46

[Article by Yu. A. Tikhomirov, candidate of technical sciences, A. M. Mastepanov, candidate of economic sciences, and S. S. Kvardakov, engineer, All-Union Scientific Research Institute of KTEP [not further identified], USSR State Planning Committee]

[Abstract] Energy conservation activities in Mutual Economic Aid countries, specifically Hungary, is aimed at planning the availability of energy and ensuring its economic use, also ensuring safe use of the energy sources. The committee established in 1982 for supervision of these activities has been organized into three main departments: one responsible for power systems design, energy consumption analysis, short-range planning, and long-range planning, one responsible for territorial balancing of energy distribution and energy management by enterprises, one responsible for improvement of the energy economy, including detection and elimination of waste. Reliable and effective energy balance accounting and reporting is most extensively done in Hungary, where also several interesting incentives have been introduced to stimulate energy conservation. The finest comprehensive energy conservation programs for specific targets have been developed in the GDR, on the basis of scientific research, while in Poland energy conservation programs are periodically set up for the various sectors of the national economy.

UDC (621.31:622.276.43.53).001.63

Comment on Article 'New Electrical Equipment in Standard Modular Cluster Pump Stations for Petroleum Industry'

18600008c Moscow PROMYSHLENNAYA ENERGETIKA in Russian No 7, Jul 88 p 47

[Article by V. S. Albokrinov, engineer]

[Abstract] Four comments are made pertaining to the redesign of standard modular cluster pump stations described by S. M. Bak and L. N. Laytkhman in PROMYSHLENNAYA ENERGETIKA No 8, 1987. 1. Standard mounting of pump sets on four reinforced-concrete pads directly on the ground, after the gravel has been preconditioned, does not meet the requirements for rotating 800-1250 kW machines driven by electric motors. Monolithic foundations have proved to be more adequate in most "Kuybyshev" petroleum pumping stations. 2. Transporting pump sets in open 2.8 m wide and 9.6 m long cars during construction work does not provide adequate protection against dirt. 3. Running power and control cables through not easily accessible places, underneath the pump sets, makes their installation and subsequent maintenance difficult. 4. The ventilation of modular cluster pump stations is primitive and thus inadequate, especially during pumping of drain water. Installation of pump sets in buildings of lighter construction on monolithic foundation should ensure reliable operation under normal rather than substandard conditions.

UDC 621.317.444

Calculation of Magnetic Systems Fabricated from Materials with Different Magnetic Properties

18600086e Novocherkassk ELEKTROMEKHANIKA in Russian No 8, Aug 88 pp 105-107

[Article by V. V. Yakovenko, V. V. Miroshnikov, and L. V. Donskaya]

[Abstract] A method exists today for magnetic field calculation in a ferromagnetic medium which involves the decomposition of the ferromagnetic material into separate elementary regions in which the modulus of the magnetization vector is identical, while its direction is dependent on the resulting field strength in the elementary region under analysis. The calculation method proposed in this study eliminates the need to use certain variables in this calculation process and rather employs reference data on the parameters of the magnetization function and the hysteresis loop of the magnetic material. The modulus of the magnetization vector in each elementary region is assumed to be constant in this case as well, while its direction is such that the projection of the magnetization vector in the direction of the resulting field vector in the given elementary section is determined by a function of the material magnetization and the field strength for the specific magnetic material under consideration. The theoretical analysis posits the existence of a permanent magnet producing a constant magnetic field in a region that is piecewise-homogeneous with respect to magnetic properties. Several resulting field strength vectors are determined by calculation and the magnetization in each elementary region is determined by the functional relation M(H) of the ferromagnetic material for each value of h. An iteration routine is used in the analysis, and the appropriate calculations are repeated until the magnetization conditions are identical for all i. The size of the elementary region is selected so that the field created by the permanent magnet will remain virtually unchanged as the number of elementary regions is increased. An experimental test of the proposed method has demonstrated that the error in calculating the field produced by a permanent magnet surrounded by ferromagnetic bodies is less than 8-10 percent and depends on the accuracy of determination of the function M(H) for the ferromagnetic materials.

UDC 535.317.2

Gain Calculation for the Optical Unit in the Automatic Control System of the Excavation Unit of Earth-Moving Machinery
18600086a Novocherkassk ELEKTROMEKHANIKA in Russian No 8, Aug 88 pp 67-72

[Article by V.A. Lisovin]

[Abstract] Circular scanning laser referencing systems are widely used today to control and monitor the position of the excavation unit in earth-moving machinery. The most important ele- ment in the operation of the entire system is the optical unit of the photodetector which consists of a circular scanning element and an optical converter. The type of optical converter as well as the laser transmitter power level are selected based on the electromagnetic radiation power level at the outcoupling window of the element. Hence in designing such a system it is necessary to calculate the power gain of the optical unit with respect to the signal arriving from the transmitter. This study determines the power gain of the optical unit for a prescribed cylindrical laser beam power level. In view of the complexity of solving the boundary problem in electrodynamics, geometrical optics is used to determine electromagnetic field propagation through the complex interface surfaces of the optical unit. The compound section of the optical unit is the optical element which consists of a set of three surfaces including an elliptical torus, a rotating device which forms a reflecting conical surface and an outcoupling mirror. Analytic geometry and geometrical optics are used to calculate the power level at the outcoupling window of the lens. The reference signal power gain is calculated for an optical element having geometrical-optical parameters of a equals 29.3, b equals 17.74, c equal 7.98, l equals 3.03; h equals 24; equals 54 degrees n equals 1.49. A reference signal power gain of .707 was obtained for these dimensions. A model optical element was fabricated from SOL organ- ic glass using these dimensions and was used for an experimental investigation. The discrepancy between calculated and experimental data was less than 7 percent.

UDC 531.787.087.92

Magnetoelastic Pressure Transducer with Monolithic Sensor and its Mathematical Model
18600086b Novocherkassk ELEKTROMEKHANIKA in Russian No 8, Aug 88 pp 72-79

[Article by S. G. Grigoryan]

[Abstract] Magnetoelastic pressure transducers generally employ a sensitive membrane that under deformation alters the stress-strain state of the magnetoelastic sensor element. Common magnetoelectric pressure transducers employ a separate magnetic circuit and membrane that are mounted in a variety of ways in the transducer housing. The magnetoelastic pressure transducer described here is novel in that it employs a monolithic sensor in which the magnetic circuit and the membrane are manufactured as a single unit. The apertures of the magnetic circuit contain one magnetizing coil and two measurement coils. When the membrane is subjected to the pressure level under measurement, mechanical stresses are produced in the magnetic circuit that alter the mag- netic permeability of its material. This study formulates a mathematical model of such a magnetoelastic pressure transducer which is then used for its optimization. Numerical methods along are used to calculate the mechanical stresses. In formulating the model certain assumptions were made, in- cluding an approximation of the magnetic circuit of the sensor element with distributed parameters by three equivalent circuits, an assumption that the amplitude of the current in the magnetizing coil is stabilized and that the coils operator in a no-load condition and that the magnetic field attenua- tion in the surface layer of the magnetic circuit does not change when the magnetoelastic pressure trans- ducer is under load. This model takes into account the surface effect in the sensor element as well as the three-dimensional stress-strain state of the element. The adequacy of the model was tested using sensor elements fabricated from 44NKHTYU steel at magnetization currents of 110 to 385 milliamperes at a frequency of 10 kilohertz. The sensor element membranes had a diameter of 10 millimeters and a thickness of 2 millimeters, with the magnetic circuit 3.5 and 4.5 millimeters in diameter respectively with an aperture diameter below the winding of 3.5 millimeters. The magnetizing coils of the sensor elements contained 20 turns while the measurement coils contained 55 turns. In the theoretical analysis the mechanical stress components for a given measured pressure were calculated by the finite element method using a standard program on an ES1045 computer. A three-dimensional formulation of the problem in elasticity theory is used with the elements in the form of rectangular and triangular prisms. The Newton method was used to solve the equation sets on a computer. The maximum discrepancy between experiment and calculation was less than 20 percent, which confirms the adequacy of the model. The most appropriate material for monolithic sensor elements is 44NKHTYU steel which has superior elasticity properties and impact viscosity as well as acceptable magnetoelastic sensitivity and resistance to corrosion. The magnetoelastic pressure transducer with such an element has a refined error factor of less than 1 percent and is suitable for series manufacture.

UDC 621.315.2.016:2.621.317.333.4:534.6

Calculation of the Acoustic Field from Electrical Discharge in an Underground Cable Line
18600086c Novocherkassk ELEKTROMEKHANIKA in Russian No 8, Aug 88 pp 92-94

[Article by A. A. Pirozhnik]

[Abstract] In employing an acoustic method to determine equipment parameters and select a technique for fault localization on a cable line it is necessary to know

the spatial distribution and frequency spectrum of mechanical oscillations in the soil that occur in the search region. This study carries out an experimental investigation of the spatial and temporal shifts of the jacketing on an experimental cable section due to electrical discharge between the conductor and the jacketing from a capacitor bank in order to develop a mathematical model of the radiator and also provides a calculation of the acoustic field over the cable fault site. The calculation data suggest that the cable jacketing shift is localized in the discharge region and diminishes by more than an order of magnitude at a distance equal to the jacketing diameter, while the active shift zone does not exceed half the diameter of the cable jacketing. Since the soil oscillations are determined at distances substantially exceeding the jacketing diameter the calculation model is represented as a "expansion center" point source. Such a model is valid if its dimensions are small compared to the radiated wavelength. This imposes constraints on the frequency range in which the point model is acceptable. The range determined is in good agreement with the radiated frequency spectrum. With electrical discharge in the cable the spectrum of radiated frequencies is largely determined by the zero to two kilohertz range and is independent of the position of the discharge channel. The calculation data also suggest that the vertical amplitude displacement component is sharply localized at the fault site in an actual frequency range of 0 to 1 kilohertz with an expressed maximum at 0.5 kilohertz. The 0.02 to 1.0 kilohertz range is recommended accounting for the audible spectrum. This study suggests that when electrical discharge is present between the conductor and jacketing of a cable, the jacketing can be represented as a point model with an actual radiated frequency range of 0 to 2 kilohertz, and when the acoustical method is used for fault localization in cables it is most advisable to design the sensor to detect the vertical displacement component over an operational frequency range of 20 to 1000 hertz.

UDC 621.373.826

Error Involved in Determination of Coordinates of Energy Center of Laser Beam During Failure of Matrix-Array Elements in Instrument Transducer
18600009a Moscow IZMERITELNAYA TEKHNIKA in Russian No 7, Jul 88 pp 19-20

[Article by S. K. Ilin]

[Abstract] Determination of the energy distribution over the cross-section of a laser beam and particularly of the location of the energy center with any type of matrix-array instrument transducer is analyzed for accuracy, considering the possibility of failure of matrix-array elements during the measurement. The geometrical center of the laser beam cross-section is selected as the origin of coordinates and the energy distribution is assumed to be symmetric so that its center coincides with the origin of coordinates. The apparent shift of the energy center upon failure of one transducer element and then more elements in other rows is calculated first for a uniform energy distribution and then for a Gaussian energy distribution of laser beam energy over the field of a 16x16 transducer matrix-array. Figures 2; references 3: Russian.

UDC 535.247.4:621.383.52

Compensation for Temperature Dependence of Spectral Sensitivity of Photodiode in Pulse-Signal Photometer
18600009b Moscow IZMERITELNAYA TEKHNIKA in Russian No 7, Jul 88 pp 20-22

[Article by Ye. V. Lesnikov, N. V. Nikitin, N. I. Bespalov, and A. V. Shilin]

[Abstract] Silicon photodiodes are recommended for high-precision measurement of the energy in single or periodically repetitive light pulses on account of their high sensitivity and long lasting stability, but the temperature dependence of their spectral sensitivity needs to be compensated as an alternative to less desirable thermostatic control. Maintenance of a constant temperature above the ambient one lowers the threshold sensitivity of such a device and, therefore, compensation by the temperature dependence of another parameter is preferable. The voltage drop across a photodiode conducting a fixed forward current is such a parameter, its temperature dependence being linear. A compensator on this basis with conversion of voltage amplitude to time interval includes a storing capacitor and an integrator, the maximum integrator output voltage being proportional to the stored charge and thus to energy of an incident light pulse. It also includes a discharge-current generator which feeds the capacitor through a trigger-controlled switch upon incidence of a light pulse on the photodiode, a measuring-current generator (voltage source with high-resistance series resistor) which feed the photodiode through two trigger-controlled switches during discharge of the capacitor and which measures the photodiode temperature by temperature-to-voltage conversion, a comparator which indicates the beginning of capacitor discharge and drives the triggers, a synchronizer, an amplifier on a K153UD5 operational-amplifier integrated-circuit chip minimally sensitive to temperature drift, and an adder which adds a constant voltage to the voltage proportional to the photodiode temperature so that the algebraic sum of both voltages determines the capacitor discharge current. Figures 1; references 6: Russian.

UDC 53.088:536.51:534-8

Errors of Resonance Ultrasonic Thermometers with Phase Analysis of Echo Signal
18600009c Moscow IZMERITELNAYA TEKHNIKA in Russian No 7, Jul 88 pp 35-37

[Article by Ya. T. Lutsik, P. G. Stolyarchuk, R. I. Chekh, and I. S. Likhnovskiy]

[Abstract] Resonance ultrasonic thermometers with phase analysis of the echo signal are analyzed for errors, such an instrument including a magnetostrictive transducer which converts a modulated radio pulse into an acoustic signal and a resonant sensor which reflects a sinusoidal acoustic echo signal back to the transducer for conversion into electric signals. The radio pulse, with a variable duty factor, is generated by an oscillator tunable to the resonance frequency of the sensor and is modulated before it enters the transducer. The electric signals from the transducer are shaped into square-wave pulses by an amplifier-limiter. These pulses proceed to a pulse group discriminator which includes a comparator of pulse groups with a reference signal and an integrator of opposite-polarities pulse groups. From here signals proceed to a control integrator which tunes the oscillator and to a null indicator, both this indicator and the oscillator feeding a frequency meter. While only the error which depends on the degree of noise suppression at the amplifier-limiter input is a systematic one, inasmuch as a sinusoidal echo signal has been converted into square-wave pulses whose volt• second area is an information-carrying parameter, all the other errors are random ones: error due to variation of the sensor Q-factor and consequently of the sensor resonance frequency, error due to temperature drift of pulse integrator and control integrator characteristics, error of the null-indicator threshold, error due to oscillator frequency instability, and error of oscillator frequency measurement. Figures 2; references 7: 2 Russian, 5 Western (2 in Russian translation).

UDC 535.321

Study of Optical Fibers With Aid of Thermoplastic Attenuated-Total-Reflectance Elements
18600011a Leningrad OPTIKO-MEKHANICHESKAYA PROMYSHLENNOST in Russian No 6, Jun 88 (manuscript received 11 Aug 87) pp 1-3

[Article by L. N. Kapitanova, V. M. Zolotarev, Yu. N. Kondratyev and M. A. Sevbo]

[Abstract] The advantages of determining the optical characteristics of macro-disperse media by the method

of attenuated total reflectance are that this method does not require special preparation of specimens and yields adequately informative spectra, the main problem in the case of fibers being the need to determine the contribution of individual segments to the resultant ATR spectrum. Experimental study of optical fibers reduces, accordingly, to analysis of the light reflected by a curved boundary between two media. Such a study was done with the aid of a 60-deg Dove prism made of thermoplastic glass. A dense bundle of parallel fibers coated with SIEL 159-167 siloxane protective-reinforcing compound was laid in a single row on the prism face exposed to incident light at a 72 deg angle, solid contact between fibers and prism surface having been ensured by heating to 80 deg C. Measurements were made by the ATR method with an Elmer-Perkin 580 spectrometer in polarized 1300-700 cm^{-1} light and also by the transmission method. Processing of both spectra, in accordance with the Bouguer-Lambert-Beer law and the K-K relation respectively, yielded nearly the same values for the optical characteristics of SIEL 159-167 siloxane films cured at 250 deg C for 3 h and then cast on Teflon-4 or on pressed KVch (quartz?) substrates. Figures 2; tables 1; references 10: 6 Russian, 4 Western (1 in Russian translation).

UDC 532.317:1:331.015.11

Effectiveness of Using Circular and Square Fiber Bundles for Visual Search
18600011b Leningrad OPTIKO-MEKHANICHESKAYA PROMYSHLENNOST in Russian No 6, Jun 88 (manuscript received 12 Jun 87) pp 13-16

[Article by Yu. V. Alekseyev and P. A. Mikheyev]

[Abstract] An adaptive detection-probability model is constructed for visual search of objects on moving images within a circular or square field of vision with the aid of respectively circular or square bundles of optical fibers. Search within a narrow diametrical strip is found to be somewhat more efficient than search over the entire circular field of vision, search over a square field of vision being more efficient than search over a circular one according to most search strategies and rectangular fiber bundles with square end faces being therefore preferable. Figures 3; references 5: Russian.

UDC 621.383.8:522.617.538.81

Determination of Image Converter Characteristics by Methods of Coherent Optics
18600011c Leningrad OPTIKO-MEKHANICHESKAYA PROMYSHLENNOST in Russian No 6, Jun 88 (manuscript received 18 Jun 87) pp 16-18

[Article by V. D. Bakhtin, G. I. Bryukhnevich, V. G. Vakulik, V. V. Konichek and M. G. Sosonkin]

[Abstract] Image processing by methods of coherent optics is proposed for determination of two characteristics of an image converter, namely its noise spectrum and the dependence of its transfer ratio on the complex space frequency. Following a comparative analysis of noncoherent and coherent illumination through a linear space-invariant optical system, coherent illumination of a test object with an apriori known space spectrum rather than by a point test source is selected so that both image converter characteristics can be determined simultaneously. An analog coherent-optics spectrum analyzer with a spherical lens is used for processing a long series of images of the test object, such a lens being capable of Fourier-transforming the field distribution over its aperture. Figures 4; references 4: 2 Russian, 2 Western (both in Russian translation).

UDC 621.383.814:621.385.832.088.8

X-Ray Image Converter on Microchannel Plates
18600011d Leningrad OPTIKO-MEKHANICHESKAYA PROMYSHLENNOST in Russian No 6, Jun 88 (manuscript received 27 Oct 87) pp 23-24

[Article by A. M. Bonch-Bruyevich, V. N. Ivanov, V. A. Matusevich, I. Ye. Medvedeva, A. M. Tyutikov and A. L. Shilov]

[Abstract] A prototype x-ray image converter was designed and built with micro-channel plates instead of conventional photocathode and amplifier, the aim being a higher resolution desirable in medical diagnostics and industrial defectoscopy. It is essentially a vacuum tube with a 1.3 mm thick microchannel-plate photocathode, a 0.85 mm thick microchannel-plate amplifier, and a cathodoluminescent glass screen 20 mm in diameter inside a glass envelope, the latter having a 0.3 mm thick titanium inlet window for hard x-rays, a glass outlet window, and sealed holes for electrical lead wires. The microchannel plates have been each separately cleaned of gas prior to assembly and heat treatment at 300 deg C under vacuum for 20 h. The distance between them is 0.1 mm and the distance from the second one to the screen is 1 mm, voltages of 100 V and up to 4 kV having been applied across the respective gaps for performance evaluation tests. As radiation source served an RYeIS-I x-ray tube with copper anode operating at a voltage of 45 kV. The dependence of the screen luminance on the screen-to-amplifier voltage across the 1 mm gap was determined on the basis of measurements with a luxmeter and a voltmeter in a dark room. The resolution of this converter was checked with a special x-ray focusing chart and found to be about 10 lines/mm. Figures 3; references 4: 3 Russian, 1 Western.

UDC 681.327.68:778.38

Holographic Random-Access Memory
18600011e Leningrad OPTIKO-MEKHANICHESKAYA PROMYSHLENNOST in Russian No 6, Jun 88 (manuscript received 20 Jul 87) pp 24-27

[Article by A. P. Grammatin, V. K. Gusev, Ye. V. Dolgova, Ye. A. Zimoglyadova, V. N. Mitsay, A. A. Novikov, V. M. Pankratov, V. G. Somov, V. B. Fedorov and B. M. Yurchikov]

[Abstract] A holographic high-capacity high-speed random-access memory has been developed which consists of a holographic data read-in device with 16 optoelec-

tronic data-carrier frames and a holographic data read-out device with two optoelectronic frames, each separately energized and controlled. The read-in device is built with standard components and operates in the start-stop mode. The read-out device operates with a He-Ne laser and two pairs of rotating mirrors which guide the laser beam to an electrooptic deflector and from the latter to a projector respectively. The deflector consists of a coordinate deflection system behind a telescope with a half-wavelength phase plate in front, an angular deflection system behind a collimating objective, and a focusing objective for the projector. The performance characteristics of this holographic memory are: carrier capacity 3.2 Mbit, read-in rate 1-16 kbit/s, read-out rate 10 Mbit/s, probability of read-out error lower than 10^{-9}, cassette capacity 5.2 Mbit, time of random access to data file 0.1 ms per cassette. Figures 3; references 7: 4 Russian, 3 Western.

UDC 621.37.2.8.029.7

Instrument for Measuring Losses in Planar Optical Waveguides

18600011f Leningrad OPTIKO-MEKHANICHESKAYA PROMYSHLENNOST in Russian No 6, Jun 88 (manuscript received 21 Jul 87) pp 32-33

[Article by E. A. Arutyunyan, S. Kh. Galoyan, L. B. Glebov and N. V. Nikonorov]

[Abstract] An instrument for high-precision measurement of losses in planar optical waveguides has been developed which operates with an LG-52 He-Ne laser. Its components are a semitransparent beam-splitting mirror, two opaque mirrors, two lead-in prisms made of TF-5 glass, a lead-out prism made of TF-5 glass, two attenuating filters, and two FD-24K photodiodes. All components are mounted on a common base and the latter can be mounted on an optical bench. The two lead-in prisms are clamped to the waveguide in a fixed position, while the lead-out prism in the middle can be shifted to any point on the waveguide by means of a micrometer screw and with the two photodiodes. The main advantage of this instrument over existing ones is that fluctuations of the laser radiation and reproducibility of the coupling of the movable prism need not be monitored, the main source of measurement error being imperfect symmetry of that prism. The performance characteristics of the instrument are: spectral range 400-700 nm, range of refractive index in waveguide 1.5-3.0, loss sensitivity 0.1 dB/cm, precision of loss measurement 0.1 dB/cm. Figures 1; references 5: 2 Russian, 3 Western.

UDC 681.7.037

Optical-Grade Polymer Material 'Allur'

18600011g Leningrad OPTIKO-MEKHANICHESKAYA PROMYSHLENNOST in Russian No 6, Jun 88 (manuscript received 8 Oct 87) pp 34-35

[Article by L. B. Vladimirova, I. A. Guseva, N. N. Alekseyev and G. S. Dedovets]

[Abstract] An optical-grade colorless and transparent glassy polymer material on the basis of an allyl carbonate (DEGbAK, USSR Patent No 1,055,745 Class COSF 18 March 1982) has been developed in the USSR for "Varilux" glasses and high-grade precision optics with characteristics almost identical to those of Nouryset-200 produced in Netherlands and MR-30 produced in Japan. This material, "Allur", can be produced only by homopolymerization of that allyl carbonate and subsequent copolymerization of the latter with another monomer such as methyl methacrylate in the presence of a catalyst containing a mixture of peroxides and with stepwise heating from 50 to 100 deg C. Its density is 1.32 g/cm^3 at 25 deg C, its Brinell hardness is 118 MPa, its Wick softening temperature is not lower than 220 deg C under a 50 N load, and its refractive index n_D is 1.500 at 25 deg C. Its transmission coefficient is 089-0.92 for 540-550 nm light, 0.25 for 340 nm ultraviolet radiation, and 0.01 for vacuum ultraviolet radiation. Eye glasses as well as other lenses and also mirrors of this material are produced by free casting into molds. The material can also replace heavier and more brittle optical-grade silicate glass for large special devices. Tables 1; references 7: Western.

UDC 621.315.591

Characteristics of InP-MOS Solar Cells at High Density of Solar Radiation Power

18600013b Ashkhabad IZVESTIYA AKADEMII NAUK TURKMENSKOY SSR: SERIYA FIZIKO-TEKHNICHESKIKH, KHIMICHESKIKH I GEOLOGICHESKIKH NAUK in Russian No 4, Sep-Oct 88 (manuscript received 4 May 87) pp 35-38

[Article by O. Gazakov, A. Kh. Orazberdyyev and Ya. Charyyev, Institute of Engineering Physics, TuSSR Academy of Sciences]

[Abstract] An experimental study of metal-(n-In_2O_3)-InP structures for solar cells was made, its purpose being to determine the effects of heavy solar radiation power on their electrical and load characteristics. Diodes with such an MOS structure were built on n-InP crystals with a donor concentration of 10^{23} m^{-3} and on P-InP crystals with an acceptor concentration of 10^{22} m^{-3} grown by the Czochralski method. The crystals were etched with Br plus $4C_2H_5OH$ mixture, rinsed, dried, and annealed at a temperature of 700 K for 10 min in an atmosphere of dry oxygen. They were then coated (surface area 3 cm^2) under vacuum with a 10 nm thick semitransparent metal layer (Al,Ni,Au), on which an E-form 10 nm thick metal layer was deposited for better current conduction. The oxide interlayer was 1.5-5 nm thick. Reverse current and efficiency, also the current-voltage characteristic including open-circuit voltage and short-circuit current, were measured with the density of solar radiation power varied over the 0-75 W/cm^2 range in 0.075 W/cm^2 steps. Measurements were made over a period of two years, for a determination of aging effects. The current-voltage characteristic was found to change irreversibly upon exposure to solar radiation of higher than 3.75 W/cm^2

power density, with both open-circuit voltage and short-circuit current eventually dropping sharply. Cells with thick oxide interlayer were found to deteriorate most. Evidently high radiation flux intensity combined with an attendant temperature rise and drift of oxygen atoms, also of impurity atoms, stimulates build-up of the oxide layer into the InP crystal and eventual breakdown of that layer. Figures 1; references 4: 3 Russian, 1 Western (in Russian translation).

UDC 621.315.592

Thermal Activation Methods of Determining Parameters of Local Levels in Wide-Band Semiconductors

18600013c Ashkhabad IZVESTIYA AKADEMII NAUK TURKMENSKOY SSR: SERIYA FIZIKO-TEKHNICHESKIKH, KHIMICHESKIKH I GEOLOGICHESKIKH NAUK in Russian
No 4, Sep-Oct 88 (manuscript received 28 Oct 87) pp 39-47

[Article by G. Garyagdyyev, Turkmen Polytechnic Institute]

[Abstract] Two problems arising in development and design of photodetectors with wide-band semiconductors such as II-VI compounds are considered, the problem of establishing the physical limitations on photosensitivity related to intrinsic defect levels and impurity levels followed by the problem of reliably determining the parameters of these levels which in turn determine the life and the capture rate of excess charge carriers over given ranges of temperature and photoexcitation intensity. Thermal activation of photoconductivity in materials with compensated levels acting as capture centers for majority excess charge carriers is analyzed as a possible basis for reliable determination of these parameters, maximum photosensitivity being realized within a temperature range which is limited by thermal activation of photoconductivity on the low side and by thermal quenching of photoconductivity on the high side. The analysis is based on a multiband model where all centers influence the photosensitivity either directly as recombination centers or indirectly in terms of the electroneutrality condition during optically induced charge transfer between recombination centers and capture centers. The degree to which any i-type levels contribute to the increment of electrical conductivity, measure of their photoelectric activity, depends not only on collective and individual electronic-state characteristics but also on the ambient conditions including temperature and photoexcitation intensity. The process of thermal activation is analyzed with the concentration of donor capture t-levels first assumed to be low and then assumed to be high, impurity photoconductivity also later being taken into account. It has been tested on ZnS and $Mg_xCd_{1-x}Se$ crystals with compensation. Figures 5; references 15: Russian.

UDC 537.533.32

Design of Electrostatic Deflection Systems Accounting for Deflection Enhancement

18600101f Moscow RADIOTEKHNIKA I ELEKTRONIKA in Russian
Vol 33, No 10, Oct 88 pp 2169-2173

[Article by R. A. Lachashvili]

[Abstract] This study considers the electrostatic deflection systems in electron-optical devices employed in oscilloscope cathode-ray tubes where either post-deflection acceleration systems with dissipative field action or astigmatic lenses are used to enhance the deflection sensitivity of the instrument. Since the influence of these elements on beam deflection is related to their placement with respect to the deflection centers one relevant issue is determining the position of the deflection systems and the relative merits of each in specific applications. This study focuses on two specific designs: a post-deflection acceleration system that behaves as a scattering lens and an astigmatic deflection enhancement lens design. The use of astigmatic lenses to enhance deflection and for post- deflection acceleration requires compensation of beam astigmatism. A Fortran program was written for the BESM-6 computer to select the optimum relationship between the lengths of the signal and temporal deflection systems to satisfy specific application requirements of the cathode ray devices.

UDC 535.58:534

Optical Image Scanning by Acoustic Optic Light Filtering

18600101g Moscow RADIOTEKHNIKA I ELEKTRONIKA in Russian
Vol 33, No 10, Oct 88 pp 2177-2182

[Article by V. B. Voloshinov, L. A. Kulakov, and O. V. Mironov]

[Abstract] This study performs both an experimental and theoretical analysis of optical image shifts occurring from spectral filtering in the visible range by means of a paratellurite acoustooptic crystal filter. The physical operating principles of acoustooptic filters are illustrated by a vectorial mathematical analysis and it is determined that the dispersion, which is attributable to the chromatic aberration of the instruments, results in image scanning at the filter output when the device is tuned. From the practical viewpoint this scanning process is undesirable, since the position of the photodetector analyzing the image is always fixed with respect to the incident light. The angular image shifts are recorded by tuning the filter through the visible range and it is

determined that partial compensation of the angular shifts of the optical image can be achieved by proper selection of the geometric dimensions and configurations of the acoustooptic cell containing the paratellurite crystal. The research further suggests that image displacements in the direction of light beam propagation can be compensated by means of appropriate correction optics or other traditional methods. Displacements in the orthogonal direction can be significantly reduced by proper selection of the acoustooptic cell configuration. Such shifts can also be taken into account in the electronic processing of signals taken from the photodetector array.

UDC 621.382.7.029.6

I-E Characteristics and Nonlinear Properties of Indium Phosphide Gunn Diodes in Strong Microwave Fields

18600101j Moscow RADIOTEKHNIKA I ELEKTRONIKA in Russian
Vol 33 No 10, Oct 88 pp 2211-2214

[Article by V. I. Borisov, A. L. Galanin, V. Ye. Lyubchenko, A. S. Rogashkov, and A. A. Telegin]

[Abstract] This study analyzes the IV characteristics as well as certain nonlinear properties of Gunn diodes fabricated as honeycomb structures from epitaxial InP films grown by the gas transport method on heavily-doped substrates. The electron concentration and mobility as well as the contact resistance were measured in each specimen by the magnetic resistance method. The dependence of the IV characteristic in the negative differential conduction range on the bias voltage applied simultaneously with the microwave field suggests that the formation of static domains due to doping irregularities and current diffusion effects near the cathode contact play a significant role and make it impossible to achieve the maximum current density predicted by theory. The study also employs an existing technique to investigate the nonlinear properties of Gunn diodes in the 36 to 40 GHz range, particularly frequency detection and multiplication. Conversion with a 5 dB gain was achieved as well as a specific sensitivity of minus 82 dBm. Two important features of InP diodes were discovered in the course of the studies that differentiate these from GaAs diodes, specifically the capacity to generate microwave oscillations at an electron concentration of approximately 10 exp17 cm-3 in the active layer and the capacity for substantial heating of the active layer cathode region, which is responsible for the characteristic changes in the IV characteristic.

Foreign Broadcast Information Service (FBIS) and Joint Publications Research Service (JPRS) publications contain political, economic, military, and sociological news, commentary, and other information, as well as scientific and technical data and reports. All information has been obtained from foreign radio and television broadcasts, news agency transmissions, newspapers, books, and periodicals. Items generally are processed from the first or best available source; it should not be inferred that they have been disseminated only in the medium, in the language, or to the area indicated. Items from foreign language sources are translated; those from English-language sources are transcribed, with personal and place names rendered in accordance with FBIS transliteration style.

Headlines, editorial reports, and material enclosed in brackets [ ] are supplied by FBIS/JPRS. Processing indicators such as [Text] or [Excerpts] in the first line of each item indicate how the information was processed from the original. Unfamiliar names rendered phonetically are enclosed in parentheses. Words or names preceded by a question mark and enclosed in parentheses were not clear from the original source but have been supplied as appropriate to the context. Other unattributed parenthetical notes within the body of an item originate with the source. Times within items are as given by the source. Passages in boldface or italics are as published.

SUBSCRIPTION/PROCUREMENT INFORMATION

The FBIS DAILY REPORT contains current news and information and is published Monday through Friday in eight volumes: China, East Europe, Soviet Union, East Asia, Near East & South Asia, Sub-Saharan Africa, Latin America, and West Europe. Supplements to the DAILY REPORTs may also be available periodically and will be distributed to regular DAILY REPORT subscribers. JPRS publications, which include approximately 50 regional, worldwide, and topical reports, generally contain less time-sensitive information and are published periodically.

Current DAILY REPORTs and JPRS publications are listed in *Government Reports Announcements* issued semimonthly by the National Technical Information Service (NTIS), 5285 Port Royal Road, Springfield, Virginia 22161 and the *Monthly Catalog of U.S. Government Publications* issued by the Superintendent of Documents, U.S. Government Printing Office, Washington, D.C. 20402.

The public may subscribe to either hardcover or microfiche versions of the DAILY REPORTs and JPRS publications through NTIS at the above address or by calling (703) 487-4630. Subscription rates will be provided by NTIS upon request. Subscriptions are available outside the United States from NTIS or appointed foreign dealers. New subscribers should expect a 30-day delay in receipt of the first issue.

U.S. Government offices may obtain subscriptions to the DAILY REPORTs or JPRS publications (hardcover or microfiche) at no charge through their sponsoring organizations. For additional information or assistance, call FBIS, (202) 338-6735,or write to P.O. Box 2604, Washington, D.C. 20013. Department of Defense consumers are required to submit requests through appropriate command validation channels to DIA, RTS-2C, Washington, D.C. 20301. (Telephone: (202) 373-3771, Autovon: 243-3771.)

Back issues or single copies of the DAILY REPORTs and JPRS publications are not available. Both the DAILY REPORTs and the JPRS publications are on file for public reference at the Library of Congress and at many Federal Depository Libraries. Reference copies may also be seen at many public and university libraries throughout the United States.

END OF FICHE DATE FILMED

12 JUNE 89